Available online at www.sciencedirect.com
SCIENCE DIRECT®
C. R. Physique 6 (2005) 487–499
COMPTES RENDUS PHYSIQUE
http://france.elsevier.com/direct/COMREN/

Aircraft trailing vortices/Tourbillons de sillages d'avions

Airplane trailing vortices and their control

Jeffrey Crouch

Boeing Commercial Airplanes, Seattle, USA

Available online 5 July 2005

Abstract

Airplane trailing vortices are examined under natural and forced conditions. Control strategies are presented, which aim to reduce the potential for severe upsets resulting from encounters with the vortices. These range from passive control, using spanload modifications, up to active control, using control-surface oscillations. Flight-simulator results are used to judge the effectiveness of the different control strategies. Active control is shown to be effective for breaking up the trailing vortices, and for reducing the potential for severe vortex-encounter upsets. Stability theory is used to explain the mechanisms underlying this form of control. ***To cite this article: J. Crouch, C. R. Physique 6 (2005).***

Résumé

Tourbillons de sillages d'avions et leur contrôle. Les tourbillons de sillages d'avions sont examinés sous l'angle de leur contrôle. Diverses stratégies visant à réduire les conséquences de la rencontre d'un avion avec les tourbillons d'un avion qui le précède sont ainsi analysées. Ces stratégies couvrent le cas d'un contrôle passif, basé uniquement sur une modification du plan de voilure, jusqu'à celui d'un contrôle actif consistant à faire osciller certaines surfaces portantes. L'efficacité de ces approches est évaluée à partir des résultats d'un simulateur de vol. On montre que le contrôle actif réduit significativement le danger potentiel de l'interaction avion/sillage quand ce contrôle permet de faire interférer de manière destructive les tourbillons. Les mécanismes physiques sous jacents à cette méthode de contrôle sont explicités. ***Pour citer cet article : J. Crouch, C. R. Physique 6 (2005).***

Keywords: Vortices; Vortex breakup; Active control; Vortex encounters; Instability; Transient growth; Floquet theory

Mots-clés : Tourbillons ; Sillages d'avions ; Contrôle ; Instabilités ; Croissances transitoires ; Théorie de Floquet

1. Introduction

Trailing vortices are a natural byproduct of airplanes, and other vehicles, with finite-span lifting wings. Lift is generated by pressure differences on the upper and lower surfaces of the wings. These pressure differences lead to the creation of vortices that trail behind the airplane and persist well downstream of the vehicle. The vortices (sometimes referred to as wake vortices, or wake turbulence) are characterized by a rotational flow field, analogous to a set of tornados turned sideways with their cores aligned in the flight-path direction. The circulation strength of the vortices is proportional to the total lift (which supports the airplane weight), and inversely proportional to the vortex span (which depends on the geometric wing span and the distribution of lift along the wings) and the airplane speed.

E-mail address: jeffrey.d.crouch@boeing.com (J. Crouch).

1631-0705/$ – see front matter
doi:10.1016/j.crhy.2005.05.006

Practical interest in trailing vortices is motivated by their potential impact to following airplanes that might encounter them. As an airplane flies into the vortices of another aircraft it can experience a significant upset. This can result in the rapid rolling of the airplane due to the rotational flow, and/or a drop in the airplane's altitude. Depending on the severity of the upset and the proximity to the ground, a vortex encounter can be a safety hazard. This is a critical issue for airplanes when arriving to and departing from airports.

In order to avoid unsafe encounters near the ground, regulators have imposed airplane separation requirements for operations under instrument flight rules. The separations allow time for the vortices to be carried away from the flight path by the self induction of the rotational flow or by atmospheric currents. The separation time also allows for some amount of natural decay or breakup to occur. These separations have proven to be safe; however, they contribute to airport delays and reductions in airport capacity. Thus, the ability to minimize or destroy the vortices would be of significant benefit to air-traffic capacity in the airport terminal area.

The practical interest in trailing vortices is also motivated by their interaction with the engine exhaust plumes, which influences both the dispersion of emissions and the long-term development of condensation trails. This is a key issue for high-altitude cruise conditions. If the vortices entrain the plume, much of the exhaust will be carried to lower altitudes. If the plume is not entrained, the exhaust stays near the flight level. Thus the long term history of the plume is tied to its interactions with the trailing vortices.

This paper focuses on airplane trailing vortices produced by flaps-down airplane configurations (such as airplanes on approach to landing) in relation to their impact on following airplanes. Given that trailing vortices are an unavoidable byproduct of airplane flight, we consider the potential for reducing the risk of an unsafe encounter by modifying or breaking up the vortices. Such control could be exploited to improve airport capacity, while maintaining the safety of the current air-traffic management system. We first consider the natural development of vortices behind a range of different flaps-down configurations. We then examine the various objectives for which control could be applied, and the potential benefits of meeting these objectives. A specific control scheme, aimed at breaking up the vortices, is then presented in detail. The basic physics of the breakup scheme are examined using a simplified model for the vortex system, coupled with an existing vortex-stability theory. Finally, an overall assessment is given for the various control schemes.

2. Natural vortex development

The structure of the trailing vortices in the near field of an airplane depends on the geometric details of the wing and the horizontal tail. The distribution of lift on the wing (in conjunction with the download on the horizontal tail) can produce a single pair of vortices, or multiple pairs of vortices. Spanloads representative of different airplane configurations are illustrated in Fig. 1. A typical flaps-up configuration has a spanload that is somewhere between elliptic and triangular (e.g., Fig. 1(a)). This

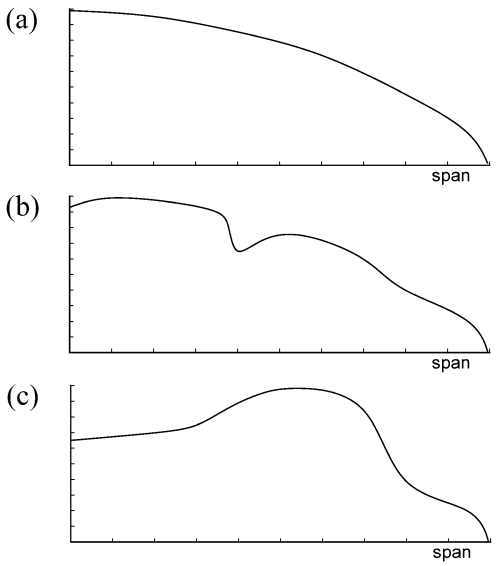

Fig. 1. Representative spanloads for aircraft with: (a) flaps up, (b) flaps down, and (c) inboard flap up and outboard flap down—each producing a different vortex system.

results in a single pair of counter-rotating vortices just downstream of the airplane. A typical flaps-down configuration carries a higher level of lift inboard (enhanced by the inboard flap), dropping to a somewhat higher level of lift outboard (enhanced by the outboard flap), then dropping to a lower level of lift outboard of the outboard flap (see Fig. 1(b)). This results in a more complex vortex system that may lead to a single vortex pair, two vortex pairs (co-rotating on each side of the airplane), or several vortex pairs (co-rotating and counter-rotating) persisting for many spans downstream of the airplane. An alternative flaps-down configuration is shown in Fig. 1(c). Here the inboard flaps are not deployed, leading to a bulge in the spanload over the region of the outboard flaps. A similar 'net spanload' could be achieved using a wing spanload similar to Fig. 1(b), with a very large download on the horizontal tail. This form of spanload leads to two vortex pairs (counter-rotating on each side of the airplane) persisting for some distance downstream.

Spanloads similar to Fig. 1(b) have been shown to produce two pairs of vortices that persist for a half to a full rotation of the co-rotating pair, which can be more than twenty spans downstream of the airplane [1,2]. The downstream persistence of the multiple vortex pairs depends on specific features of the configuration. For example, small changes to the flap system, or the horizontal-tail loading, can affect the flap-vortex lifetime. Fig. 2 shows the near-field vortex development for two different flap configurations. These results are based on Reynolds-averaged Navier–Stokes calculations, which have been shown to agree with ground-based experiments [3]. In Fig. 2(a) the flap vortices and the horizontal-tail vortices propagate toward the centerplane. Near the centerplane the vortices are mixed with their counterparts from the other side of the airplane; the mixing is enhanced by the turbulent wake of the airplane body. As a result, the flap and tail vortices are largely destroyed, leaving only a single pair of vortices beyond 15 spans. In Fig. 2(b), the flap and tail vortices also propagate toward the centerplane, but the flap vortices are not mixed out in this case. This leads to a two-pair system with co-rotating vortices persisting beyond 20 spans downstream.

The co-rotating vortex system of Fig. 2(b) can be characterized by a circulation ratio $\Gamma = \Gamma_f/\Gamma_T$ and a vortex spacing parameter $\delta_{yz} = d_{yz}/b$. The circulation values Γ_f and Γ_T correspond to the flap and tip vortices, respectively. The variable d_{yz} is the distance between the flap and tip vortices, measured in the y–z plane at a given x position. The distance b is measured between the vorticity centroids for the starboard and port wings. The coordinates x, y, z correspond to the streamwise, the spanwise, and the vertical directions, respectively. Since δ_{yz} changes with distance behind the airplane, it is helpful to define a single representative measure of the spacing, $\bar{\delta}_z$; this is defined as the value of δ_{yz} measured when the flap vortices are directly below the tip vortices (i.e., at one quarter of a rotation period). The value of Γ is primarily set by the drop in lift at the outboard edge of the inboard flap. The value of $\bar{\delta}_z$ depends on the spanwise location of the inboard-flap edge, and on the horizontal-tail

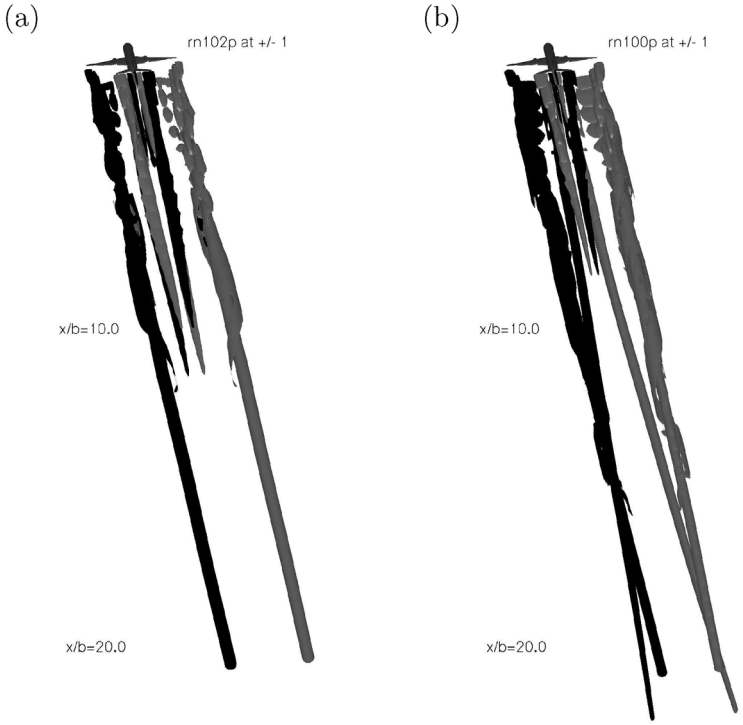

Fig. 2. Near-field wake development for two flaps-down span loads similar to Fig. 1(b) showing: (a) only tip vortices and (b) flap and tip vortices after 20 spans behind the airplane (after [3]).

loading [3]. The basic characterization of multiple-pair wakes is based on wind-tunnel wake surveys, towing-tank visualizations, and near-field CFD calculations. These have generally neglected engine-thrust effects, which are expected to be significant in flight.

A two-pair system, with counter-rotating vortices on each side of the airplane, can also be characterized by Γ and δ_{yz}; in this case, $\Gamma < 0$. The generation of significant counter-rotating vortices comes at great costs. This can be seen in Fig. 1(c), where there is a large lift loss over the inboard flap, compared to the conventional flap system of Fig. 1(b). To compensate for the lift loss, the outboard part of the wing must carry more load—resulting in an increase in the tip-vortex strength. These alterations also result in a reduction in the overall efficiency of the airplane. Most configurations will generally not have excess lift that can be forfeited over the inboard wing. When tail vortices are used to generate the counter-rotating pair, Durston et al. [4] have shown that the center-of-gravity position for the airplane is highly constrained.

3. Control objectives

In this paper, the ultimate objective of trailing-vortex control is assumed to be the alleviation of potentially severe upsets resulting from a following aircraft encountering the wake. The approaches to achieve this ultimate objective can be grouped into two categories, based on the manner in which the vortices are altered. The first category of approaches aims at breaking up the vortices by exciting large-scale three-dimensional instabilities using some form of active control. These instabilities amplify periodic perturbations to the vortex positions leading to the formation of vortex rings similar to Fig. 3(a). The second category of approaches aims to weaken or modify the structure of the vortices, or of the vortex wake as a whole. This is normally achieved through alterations to the span loading, and/or through naturally excited instabilities. An idealized example of this is given in Fig. 3(b), where the vortices are presumed to cancel each other out at some distance downstream of the airplane. In this illustration, the control is assumed to redistribute vorticity over a much larger area than would normally occur, allowing the counter-rotating vortices to cancel out.

3.1. Vortex breakup

Early efforts to break up the vortices focused on the excitation of the long-wavelength instability that exists for a pair of counter-rotating vortices. This instability was first analyzed by Crow [5], and is often referred to as the Crow instability. Crow [6], and later Crow and Bate [7], proposed a scheme to excite the Crow instability by oscillating the lift distribution to move the centroid of vorticity inboard and outboard along the wing. A scheme of this type was tested in a towing tank by Bilanin and Widnall [8]. Their study showed that the instability could be excited by a prescribed oscillation of the lift distribution. However, the level of lift oscillation required to break up the vortices (within a useful distance) was excessive.

More recent efforts to break up the vortices attempt to exploit instabilities that exist for multiple pairs of trailing vortices, as produced by airplanes with their flaps deployed. These instabilities were first analyzed in the studies by Crouch [9,10]. This analysis focused on two pairs of trailing vortices, with co-rotating vortices on each side of the airplane. The multiple vortex-pair instabilities grow up to five times more rapidly than the Crow instability, offering the potential for a more practical means of achieving the breakup. A scheme based on the excitation of these instabilities was proposed and tested by Crouch, Miller and Spalart [2]. The approach is analogous to the concepts of Crow and Bate [7] and Bilanin and Widnall [8], but the form of the forcing function is significantly different. This approach enables a more rapid breakup of the vortices, with a lower level of lift oscillation. This work is considered in greater detail in Section 5.

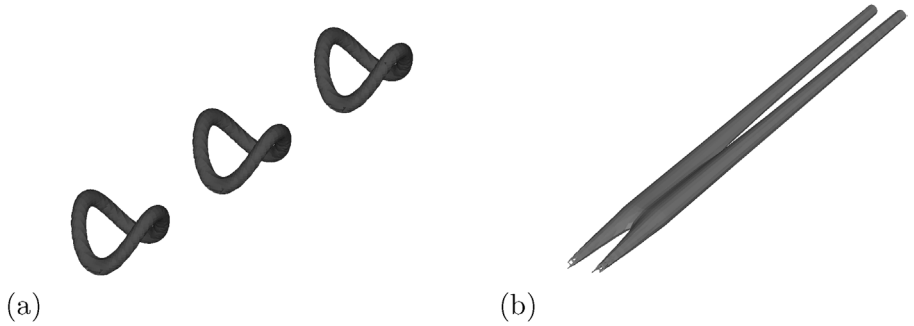

Fig. 3. Illustration of potential control objectives, leading to (a) vortex rings or (b) vortex enlargement with strength reduction.

Other recent efforts to break up airplane trailing vortices have considered a pair of counter-rotating vortices on each side of the airplane. Rennich and Lele [11] proposed a breakup scheme based on a special configuration of this vortex system. When the strengths and positions of the vortices are tuned to allow the four vortices to stay in-plane as they propagate downward, long-wavelength perturbations grow very rapidly. This leads to a rapid breakup of the vortices, with a very-small level of initial forcing. This was analyzed by Fabre and Jacquin [12], who showed that the growth rates can be orders of magnitude larger than that of the Crow instability. They also show that without active forcing, shorter-wavelength instabilities dominate leading to the demise of the weaker vortices without impacting the stronger vortices. These instability growth rates are very favorable for vortex breakup, but the vortex configurations necessary to achieve them are very difficult to realize in practice.

Fabre et al. [13] show that two vortex pairs, with counter rotating vortices on each side of the airplane, can exhibit dramatic instability growth even when the conditions proposed by Rennich and Lele [11] are not met. In these cases, the vortices tumble as the perturbations grow. This has been observed in experiments of Ortega et al. [14], Jacquin et al. [15], and Haverkamp et al. [16]. This type of instability growth can lead to rapid breakup of the weaker vortices on each side of the airplane. The time to breakup decreases as the strength of the weaker vortex pair is decreased relative to the stronger pair. After the weak-vortex breakup, the stronger vortices are left with a perturbation that is inversely proportional to their strength relative to the weaker pair. Depending on the wavelength, this perturbation can continue to grow (at a much slower rate) until the stronger vortices also break up into rings. When properly forced, this system of vortices can lead to a more rapid breakup than can be achieved with a single vortex pair. Without forcing, this system of vortices does not lead to a rapid breakup of the dominant vortices, but the altered vortices may be more benign to an encountering airplane. This is further discussed in the next section.

3.2. Vortex modification and decay

As an alternative to active control, numerous schemes have been proposed to modify the trailing vortices or to enhance their decay [17,18]. These schemes generally aim to reduce the strength of the vortices, or to enlarge the vortex cores. The vortices are modified by changes in the wing span loading, and in some cases, variations in the axial flow through drag devices or mass injection. Various wing-tip devices have also been proposed to alter or 'alleviate' the vortices by modifying the roll-up process.

For a single pair of vortices from an airplane with a given weight and speed, the vortex strengths are inversely proportional to their spacing. Thus, the circulation is decreased with an increase in the wing span. However, this combination results in reductions in the vortex descent rate, and in the natural vortex-breakup rate (under atmospheric-turbulence excitation). Thus the potential reduction in the level of upset (due to lower circulation) could be offset by an increased probability of encounter for a following airplane on the same flight path.

Ground-based experiments have shown that alterations in loading and axial flow can increase the vortex core size—thus, reducing the peak velocities in the vortices [17]. The effectiveness of these schemes at flight Reynolds numbers is largely unknown. To enhance the decay of the vortices, vorticity must be brought to the centerplane, where it can be canceled by counter-rotating vorticity from the other wing. This requires an unrealistically-large increase in the vortex-core diameter, from a typical value of less than 10% of the vortex spacing to a value near 100%. The exploitation of vortex bursting to 'destroy' the vortices has also been suggested. However, this shows little promise in practice as discussed by Spalart [19]. Significant axial flow in a vortex can lead to instability and the disruption of the vortex core. However, Ragab and Sreedhar [20] have shown that this ultimately leads to a reorganization of the vortex into a new form that is stable to further reorganization. Their study shows that it is very difficult to significantly alter airplane trailing vortices by operating on the individual vortices.

Similar to the vortex breakup efforts, the more recent attempts at vortex modification have focused on multiple vortex-pair systems. Several studies have considered the unforced development of a two-pair system, with counter-rotating vortices on each side of the airplane [4,13–16,21]. When forced, this system can lead to enhanced breakup of the vortices as discussed in the previous section. When unforced, shorter-wavelength instabilities grow most rapidly and can lead to a pinching of the weaker vortices [13,14]. The larger vortices are left in a perturbed state, with a waveform similar to a single-pair Crow instability. However, the wavelength may be too short to allow continued growth on the single pair.

If the weaker vortices do not pinch across the centerplane, the perturbations can become very large as they orbit the stronger vortices [22]. The relative magnitude of the perturbations on the stronger and weaker vortices is roughly inversely proportional to their circulations. Thus, if the weaker vortex has substantially less circulation it can become very distorted; in this case, the stronger vortex is largely unperturbed. The results of Ortega et al. [22] show that the dynamics of the counter-rotating system can lead to a factor of 3 increase in the effective vortex-core size. However, this may be accompanied by roughly a factor of 2 increase in the vortex spacing. The relative coherence of the vortices, as measured by a 'pseudo-two-dimensional kinetic energy', is reduced as a result of the instability development. The results of Durston et al. [4] suggest that the net result of the unforced counter-rotating pair is an altered pair of vortices, which might be characterized by waviness, an enlarged core, and/or some form of streamwise periodic distortion of the cores. The basic strength and centroid positions of the resulting vortices can usually be estimated from the near wake, without regard for the instabilities.

The vortex-modification approach has the advantage of being a passive form of control. However, this does not mean that there are no costs associated with this approach. The generation of a significant counter-rotating pair, for example, requires a large drop in wing loading near the body of the airplane or a large downward tail load; both of these impact the airplane efficiency, as discussed in Section 2.

4. Benefits of control

The benefits of any form of vortex control must be judged in terms of the change in probability for unacceptable upsets for encountering airplanes. This assessment involves three different elements: the probability of an encounter, the probability that a given encounter will exceed some threshold measure, and the demarcation between acceptable and unacceptable levels of upset (which will depend on the airplane's altitude). The relative effectiveness of different vortex-control strategies can be judged by estimating the worst level of upset that could be experienced by an aircraft encountering the 'controlled' vortices at a given separation distance. This effectiveness has to be weighed against the practical costs associated with the control strategy.

Earlier studies have shown that the maximum bank angle (see Fig. 4(a)) provides a good measure for the level of upset experienced by an encountering airplane [17,23]. The maximum bank angle was shown to provide the best demarcation between hazardous and nonhazardous encounters. Loucel and Crouch [24] provide a flight-simulator study of airplane encounters with trailing vortices at different stages in the vortex-breakup process. The encountering airplane is a 737-300 under the control of the autopilot. The airplane is in level flight when it encounters the vortices at a prescribed grazing angle ψ, measured in the horizontal plane. The vortices can have different pitch angles θ with respect to the flight path as shown in Fig. 4(b). These flight-simulator results provide some insight into the relative benefits of the various forms of control.

Fig. 5 shows the maximum bank angle experienced by a 737 encountering a 767-sized-aircraft wake. The first image shows results from encounters with straight vortices, for different values of ψ and θ. The results are symmetric about the $\psi = 0^\circ$ axis.

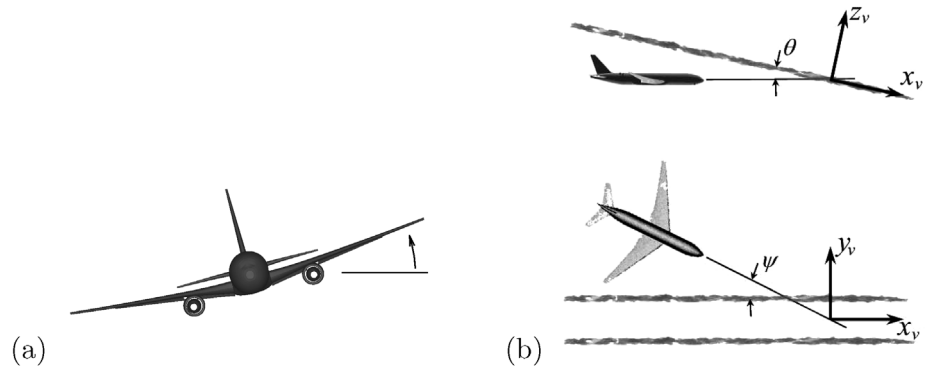

Fig. 4. Schematic showing: (a) the bank angle characterizing a vortex-encounter response, and (b) the grazing angles (ψ, θ) governing the vortex encounter (after [24]).

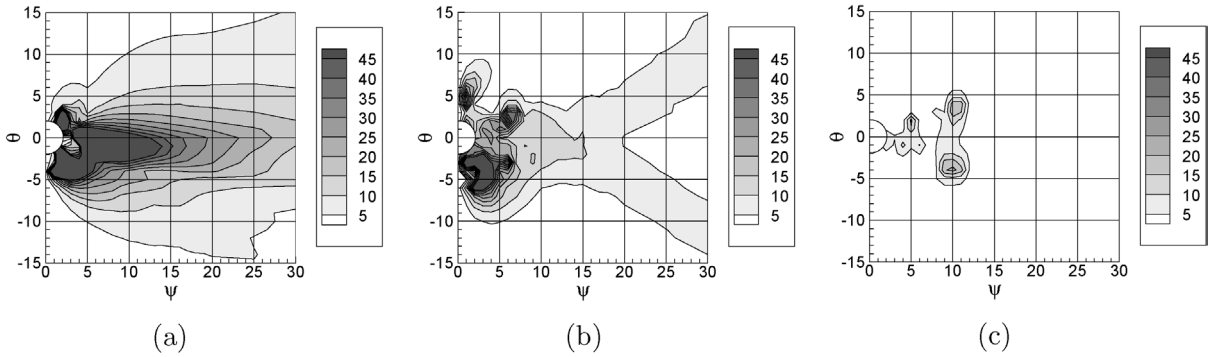

Fig. 5. Contours of maximum bank angle (degrees) experienced by a 737 aircraft encountering a 767-sized-aircraft wake with: (a) straight vortices, (b) wavy vortices ($A_v = 0.4b$), and (c) ring vortices ($T_v = 0.5$). Flight-simulator predictions for ($\widetilde{\Gamma} = 372\ \mathrm{m}^2/\mathrm{s}$, $c = 0.1b$) from [24].

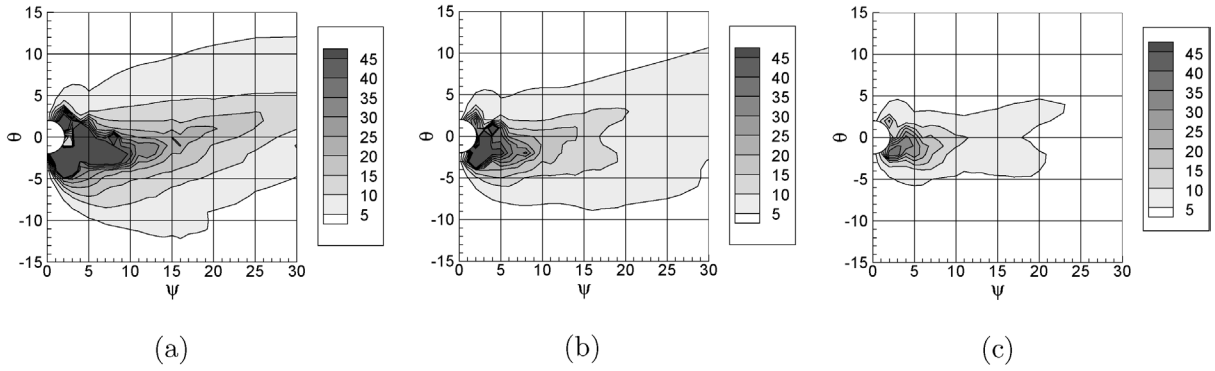

Fig. 6. Contours of maximum bank angle (degrees) experienced by a 737 aircraft encountering a 767-sized-aircraft wake with $A_v = 0.1b$ and: (a) $\widetilde{\Gamma} = 372\ \mathrm{m}^2/\mathrm{s}$, $c = 0.1b$; (b) $\widetilde{\Gamma} = 279\ \mathrm{m}^2/\mathrm{s}$, $c = 0.2b$; (c) $\Gamma = 186\ \mathrm{m}^2/\mathrm{s}$, $c = 0.2b$. Flight-simulator predictions after [24].

The maximum bank angle exceeds 5 degrees for most of the encounter angles (ψ, θ). For small values of θ, the maximum bank angle exceeds 15 degrees for all values of ψ up to approximately 30 degrees.

The effects of vortex breakup are shown in Fig. 5(b) and 5(c). Fig. 5(b) shows the maximum bank angle experienced due to encounters with wavy vortices; the shape of the vortex waviness is derived from stability theory [5,10]. The amplitude of the waviness is $A_v = 0.4b$ (where the vortices breakup into rings at an amplitude of $A_v = 0.5b$). The waviness has a dramatic effect on the vortex encounters. Most of the encounters now result in maximum bank angles of less than 5 degrees. Maximum bank angles in excess of 15 degrees are limited to encounters with grazing angles (ψ, θ) of less than about 5 degrees. Fig. 5(c) shows an even greater reduction in the levels of upset, resulting from the breakup of the vortices into rings. The vortex-ring shape is based on experimental observations, and is parameterized by a nondimensional time measured from the point of breakup. The maturity of the rings in the simulation results correspond to a nondimensional time of $T_v = 0.5$ (where the rings change aspect ratio at $T_v = 1$). Additional details are given in [24]. The vortex-ring encounters result in maximum bank angles of less than 5 degrees for almost all encounter angles. Encounter angles in excess of 15 degrees only occur in very narrow regions around $\psi = 10°$.

For comparison purposes, we also consider flight-simulator results for encounters with 'modified' vortices. The modifications are generic, and not tied to any specific modification concept. Fig. 6(a) shows the maximum bank angles experienced due to encounters with slightly wavy vortices, $A_v = 0.1b$. This level of waviness could be the result of naturally forced Crow instability (under relatively calm atmospheric conditions), or the result of some form of multiple vortex-pair instability. The vortex circulation $\widetilde{\Gamma} = 372\ \mathrm{m}^2/\mathrm{s}$, the vortex spacing $b = 36.6$ m, and vortex-core diameter $c = 0.1b$ are the same as for Fig. 5. This mild amount of waviness already has some effect on the level of upsets, as compared to Fig. 5(a). Fig. 6(b) shows the effect of a 25% reduction in the vortex strength along with a 100% increase in the vortex-core diameter. The level of upsets are significantly reduced compared to the reference case of Fig. 5(a)—although, some of the reduction is from the small level of waviness considered in the results of Fig. 6. Independent simulations show that the core size has a much smaller effect on the encounters compared to the circulation and the waviness. With a further reduction in the vortex strength ($\widetilde{\Gamma} = 186\ \mathrm{m}^2/\mathrm{s}$, which is comparable to the 737 wake strength), most of the encounter angles result in maximum bank angles of less than 5 degrees. A collection of small grazing angles, $\psi < 5°$, still results in maximum bank angles in excess of 15 degrees.

The flight simulator results show that both vortex breakup, and substantial vortex modification can reduce risks of experiencing an excessive upset due to vortex encounter. Wavy vortices result in less severe upsets compared to straight vortices. The formation of vortex rings results in a dramatic reduction in both the probability of a substantial upset and the level of the upset. A reduction in the vortex circulation can also reduce the potential for excessive upsets. However, large reductions in the circulation may be required. To match the benefit of vortex breakup (at the stage of Fig. 5(c)), the circulation must be reduced by more than a factor of 2.

5. Controlled vortex breakup

For co-rotating vortex systems, as generated by spanloads similar to Fig. 1(b), active control can be used to enhance the breakup of the trailing vortices. The basic concept is shown schematically in Fig. 7. Unsteady spanload variations are used to shift lift inboard and outboard along the wing to spatially perturb the flap and tip vortices. The prescribed perturbation shifts the flap vortices outboard as the tip vortices are shifted inboard. The relative size of the shifts is inversely proportional to the vortex circulations, resulting in a negligible movement of the vorticity centroid on each side of the airplane and negligible lift variation.

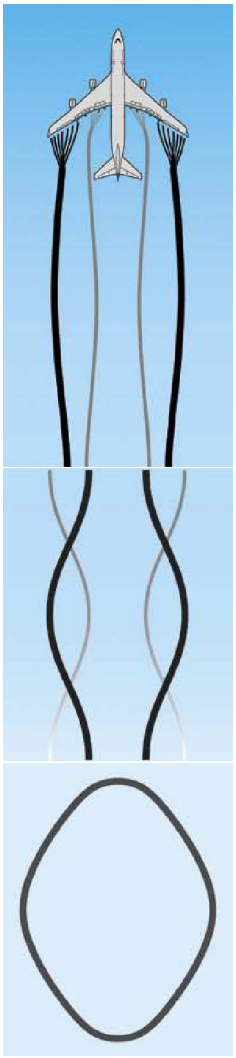

Fig. 7. Schematic showing: initial vortex perturbations, the intermediate development, and the far-field result of active control using conventional airplane control surfaces.

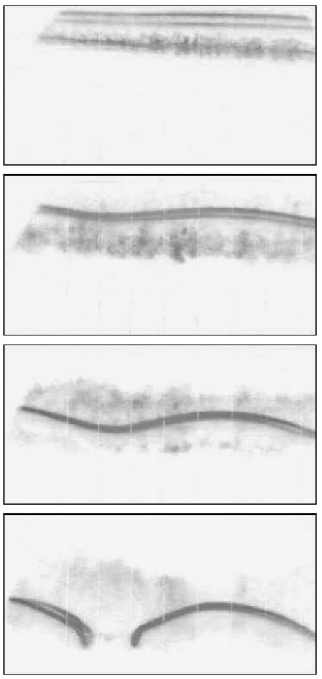

Fig. 8. Side view of trailing vortices at four different times, showing breakup into rings (from [2]). Airplane went from right to left at the top of the frame.

The perturbations are applied symmetrically about the airplane centerline, thus maintaining zero rolling moment. Any variation in the pitching moment, due to wing sweep, is trimmed out using the elevator. The frequency f of the unsteady forcing is used to control the wavelength $\lambda = V_A/f$, where V_A is the airplane speed. The wavelength is selected to excite instabilities that grow rapidly on the co-rotating vortex system [10]. If the initial forcing is large enough, these instabilities lead to a breakup of the vortices into a series of vortex rings (similar to Fig. 3(a)).

The concept was demonstrated in a water towing tank at the U.S. Navy David Taylor Model Basin [2]. A relatively small 0.9 m span model was tested in the large 15.5 m wide, 6.7 m deep, 350 m long towing facility. This enabled the study of the vortices at large distances behind the airplane (e.g., greater than 7 n miles when scaled to flight for a large airplane). The model was constructed to enable symmetric forcing of the vortex system with negligible variation in the total airplane lift. The level of forcing is measured by the amount of lift that is shifted inboard and outboard during a forcing cycle. The vortices were visualized using fluorescent dye injected at the outer edge of the inboard flap, the outer edge of the outboard flap, the wing tip, and the horizontal tail.

A side view of the vortices undergoing breakup is shown in Fig. 8. The four frames are $\tau_w = 0.5$, 1.5, 2.5 and 3.5 (with time increasing from top to bottom). The last frame is comparable to a side view of the vortex rings of Fig. 3(a). The nondimensional

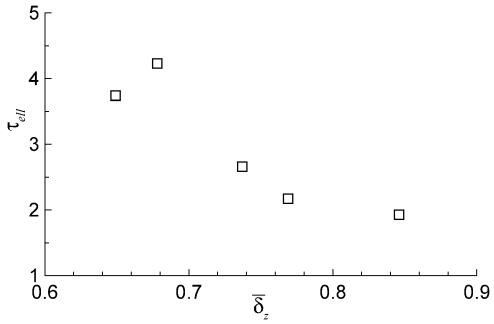

Fig. 9. Nondimensional time to breakup as a function of the vortex spacing parameter $\bar{\delta}_z$, showing greater control effectiveness with larger vortex spacing (after [2,3]).

time scale is defined as $\tau_w = t/(2\pi b_w^2/\Gamma_w)$, where b is the vortex-centroid spacing, Γ is the circulation, and the subscript w signifies quantities based on the wing vortices alone. The forcing level in this case is $\Delta C_L/C_L = 0.06$, and the wavenumber is $\alpha = 2\pi b_w/\lambda = 0.8$. This leads to a breakup into rings at $\tau_w = 3.3$. Using the common scaling based on an elliptic-spanload approximation, the breakup time is given by $\tau_{\text{ell}} \approx 2$. When scaled to flight this breakup time corresponds to less than 3 n miles behind a 747-400 on approach. For reference, the current FAA separation standards require a 5 n mile separation for a 737-sized airplane following a 747.

Active control provides an effective means for breaking up trailing vortices characterized by a co-rotating pair on each side of the airplane. The efficiency of the breakup scheme depends on the details of the wake system, and the parameters of the forcing. The towing-tank results show a strong dependence of the breakup time on the strength of the horizontal-tail vortices [2]. Stability analysis shows a negligible change in the perturbation growth on the tip vortices due to inclusion of the tail vortices. Rather, the sensitivity to the tail-vortex strength has been linked to the influence of the tail vortices on the final spacing between the flap and tip vortices, $\bar{\delta}_z$ [25]. Stronger tail vortices produce larger values of $\bar{\delta}_z$, and result in smaller breakup times. Fig. 9 shows a plot of the breakup time, measured in [2], as a function of the spacing parameter $\bar{\delta}_z$. These results are for a given wing loading, but with different settings of the horizontal-tail angle. In general, the control effectiveness drops off with smaller values of $\bar{\delta}_z$. By recasting the results in terms of $\bar{\delta}_z$, the breakup time can be estimated for different configurations, or different flow conditions—including at higher Reynolds numbers.

6. Physics of vortex-breakup

The controlled breakup of the vortices, shown in Fig. 8, results from the excitation of instabilities in the multiple-vortex-pair system. The initial stages in the instability development are governed by a simple set of equations developed in [10]. A perturbation to the vortices can be described by a disturbance vector $\phi = (\eta_1, \eta_2, \eta_3, \eta_4, \zeta_1, \zeta_2, \zeta_3, \zeta_4)^{\mathrm{T}}$, where η corresponds to a spanwise perturbation, ζ corresponds to a vertical perturbation, and the subscript signifies the vortex being perturbed (i.e., 1,2 left and right tip vortices and 3,4 left and right flap vortices). The stability equations can be written in the compact form

$$(\mathrm{d}/\mathrm{d}t)\phi = \big[\mathbf{F}(t)\big]\phi \tag{1}$$

The elements of the matrix $[\mathbf{F}(t)]$ depend on time through the changing vortex positions, as the vortices tumble downward. Thus $[\mathbf{F}(t)]$ satisfies the condition $[\mathbf{F}(t+T)] = [\mathbf{F}(t)]$, where T is the rotation period for the co-rotating pair. The vortex positions and the coefficient matrix $[\mathbf{F}(t)]$ are characterized by the circulation ratio Γ, the vortex-spacing parameter δ, and the cutoff parameter ε. The circulation ratio $\Gamma = \Gamma_f/\Gamma_T$ was discussed in Section 2. The spacing parameter is defined as the initial distance between the flap and tip vortices for a simple two-pair system (i.e., measured when the vortices are all at the same height). The cutoff parameter is part of the theoretical modeling for the vortices, and is related to the vortex core diameter [5,10]. Here, the flap and tip vortices are considered to have the same core size, and the same value of ε. The choice of ε values primarily effects the instability wavelength, but this is not significant to the key results presented here.

The growth rate for instability can be determined from Eq. (1) using the Floquet theory [10]. First, a nonsingular constant matrix $[\mathbf{A}]$ is generated by numerically integrating equation (1) over one period of the vortex rotation. Using $\phi(0) = (1,0,0,0,0,0,0,0)^{\mathrm{T}}$ as an initial condition, the resulting vector after integration provides the first column of $[\mathbf{A}]$, $a_1 = \phi(T)$. Likewise, setting the kth element of $\phi(0)$ to 1 with all others zero yields the kth column a_k. The disturbance vector after one period of evolution $\phi(t+T)$ can then be related to the disturbance vector $\phi(t)$ through the relation

$$\phi(t+T) = [\mathbf{A}]\phi(t) \tag{2}$$

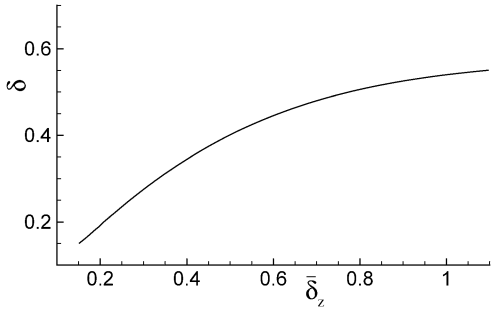

Fig. 10. Variation of the spacing parameter δ (used for modeling a two-pair vortex system) with the more-general parameter $\bar{\delta}_z$ (used to describe more-complex airplane wakes).

Introducing $\phi(t) = [\mathbf{P}]\psi(t)$, where the columns of $[\mathbf{P}]$ are unit norm eigenvectors of $[\mathbf{A}]$, Eq. (2) can be written in the form

$$\psi(t+T) = [\mathbf{P}]^{-1}[\mathbf{A}][\mathbf{P}]\psi(t) = [\mathbf{S}]\psi(t) \tag{3}$$

Assuming the eigenvalues of $[\mathbf{A}]$ are distinct, the matrix $[\mathbf{S}]$ is diagonal with the eigenvalues σ as its entries. For a given eigenvalue, $\psi(t+nT) = \sigma^n\psi(t)$, or more generally,

$$\psi(t+nT) = [\mathbf{S}]^n\psi(t) \tag{4}$$

The function ψ can be written in the normal form by introducing $\gamma = \ln(\sigma)/T$,

$$\psi(t) = \exp(\gamma t)\chi(t) \tag{5}$$

$\chi(t)$ is a periodic function and γ is the characteristic exponent. The condition for instability then has the usual form $\gamma > 0$.

The potential for transient growth can be estimated by considering the upper bound on the energy amplification for a given initial condition $\phi(0)$. The maximum amplification after one period $G(T)$, for an initial input of unit norm $\|\phi(0)\| = 1$, is

$$G(T) = \sup_{\|\phi(0)=1\|} \big\|\phi(T)\big\| = \big\|[\mathbf{A}]\big\| \tag{6}$$

Here, the vector and matrix L_2-norms are used.

This two-pair model provides a simple idealization of the more complex system of vortices produced by airplanes with flaps deployed. The flaps-down configuration typically has many vortex pairs at the tail of the airplane, as shown in Fig. 2(b). However, after a distance of approximately 5 to 10 spans downstream, the vortices evolve like a simplified two-pair system; but, a value of δ measured at the tail plane (in the many-pair system) cannot be directly related to the simplified-model δ. In order to apply the stability theory to the more complex vortex system, we determine the effective value of δ (for the simple system) that will yield a value of $\bar{\delta}_z$ to match the more complex vortex system. Using the effective δ, the simplified model provides a good estimate for the linear development of instabilities. A plot of $\bar{\delta}_z$ as a function of δ is given in Fig. 10 for $\Gamma = 0.20$. Values of $\bar{\delta}_z > 0.6$ correspond to $\delta > 0.45$ in the simple system. Values of $\delta > 0.5$ do not imply that the flap vortices start at the centerline, since δ is measured inward from the tip vortices and not from the wing-vorticity centroid.

Fig. 11 shows the stability results for the conditions $\Gamma = 0.20$, $\varepsilon = 0.05$ and $\delta = 0.35, 0.45, 0.51$, corresponding to $\bar{\delta}_z = 0.41$, 0.61, and 0.81, respectively. For the smaller values of δ, two distinct symmetric modes are observed. These are referred to as the S_1 and S_2 modes [10]. The S_1 mode is amplified for $\alpha < 1.2$ and is only weakly dependent on the separation parameter δ. This mode is a generalization of the long-wavelength Crow instability [5]. The S_2 mode exists over larger values of α, and depends more strongly on the value of δ. For $\delta = 0.35$, the S_2 mode exists for $3.2 < \alpha < 5.6$, but for $\delta = 0.45$ the mode is amplified over $1.6 < \alpha < 3.8$. For large values of δ, the S_1 and S_2 modes overlap in the neighborhood of $\alpha \approx 1$.

The maximum amplification, for any potential perturbation of unit magnitude, is given by $G(T)$. This is a measure of the total growth over one period of rotation for the co-rotating pair. Fig. 12 shows the maximum amplification factor plotted against the wavenumber α for the different values of δ. The curves show a general increase in the total amplification as δ is increased. Some of this increase is due to the increase in the period over which the amplification occurs. The minima in the curves correspond to wavenumbers where the peak amplification occurs at some fraction of a period (e.g., at $T/2$). For $\delta = 0.51$, the maximum amplification occurs around $\alpha \approx 1$. The level of amplification is substantially larger than would be expected from normal-mode growth alone. Using a linear growth rate of 0.8, over a period of $T = 3.44$, gives an amplification ratio of 16 compared to a value of around 400 due to the transient growth. The actual level of amplification will depend on the form of the initial perturbation.

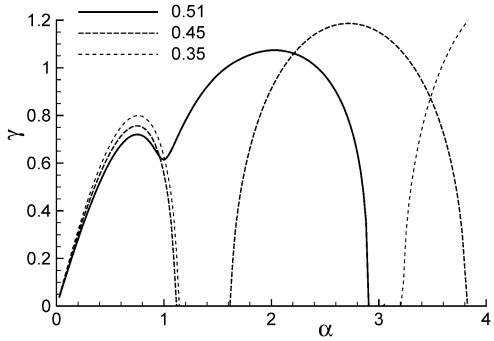

Fig. 11. Instability growth rate γ for the dominant symmetric modes as a function of the wavenumber α for: $\delta = 0.51, 0.45, 0.35$ ($\Gamma = 0.2$, $\varepsilon = 0.05$).

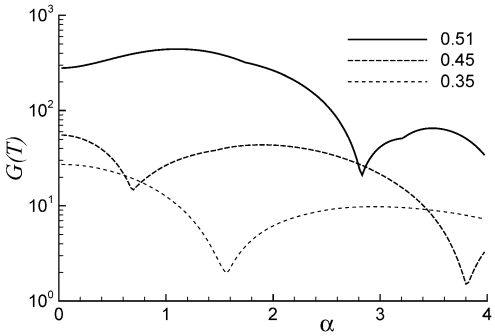

Fig. 12. Maximum amplification factors G, measured over one rotation period T, as a function of the wavenumber α for: $\delta = 0.51, 0.45, 0.35$ ($\Gamma = 0.2$, $\varepsilon = 0.05$).

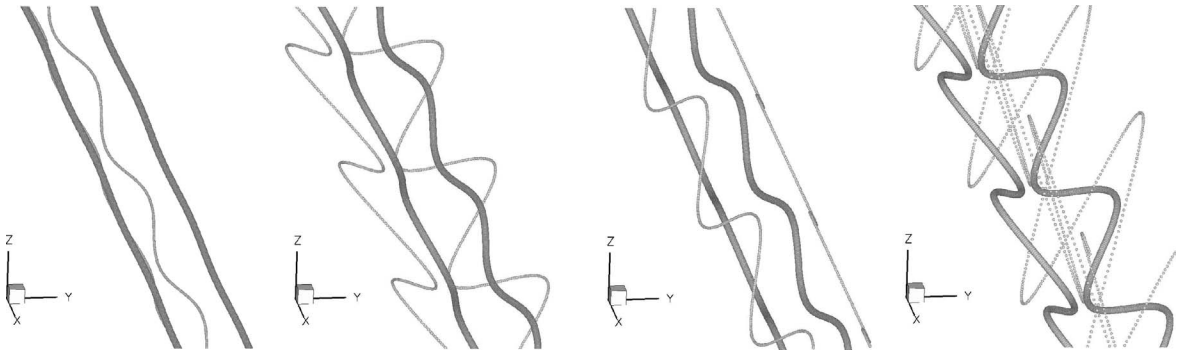

Fig. 13. Oblique view of vortices showing instability growth toward vortex breakup. Images correspond to $t/T = 1/8, 3/8, 5/8, 7/8$ for ($\alpha = 0.8$, $\Gamma = 0.2$, $\delta = 0.51$, $\varepsilon = 0.05$).

The perturbation growth for large values of δ differs from the growth for smaller values of δ in both the level of amplification and the form of the amplification. A typical transient-perturbation shape for $\delta = 0.4$ shows a change in perturbation orientation over the rotation period, which is in contrast to the S_1 and S_2 modes [10]. For $\delta = 0.51$, the perturbation mode shape follows that of the S_2 mode. Fig. 13 shows the vortices for a co-rotating pair with $\Gamma = 0.2$ and $\delta = 0.51$. The four images correspond to different times in the rotation period. The tip vortices are shown as larger filements. The perturbation was initialized by a $0.007b_w$ spanwise displacement of the tip vortices, and a $0.035b_w$ spanwise displacement of the flap vortices. This ratio is inversely proportional to the circulation ratio Γ, so the centroid of vorticity is unperturbed. Based on these initial amplitudes, the flap vortices would link before $t/T = 7/8$, or they would wrap around the tip vortices due to nonlinear effects. The tip vortices would link soon after $t/T = 7/8$, with minimal influence from the nonlinear effects on the flap vortices. The overall mode shapes of Fig. 13 are similar to the S_2 mode [10].

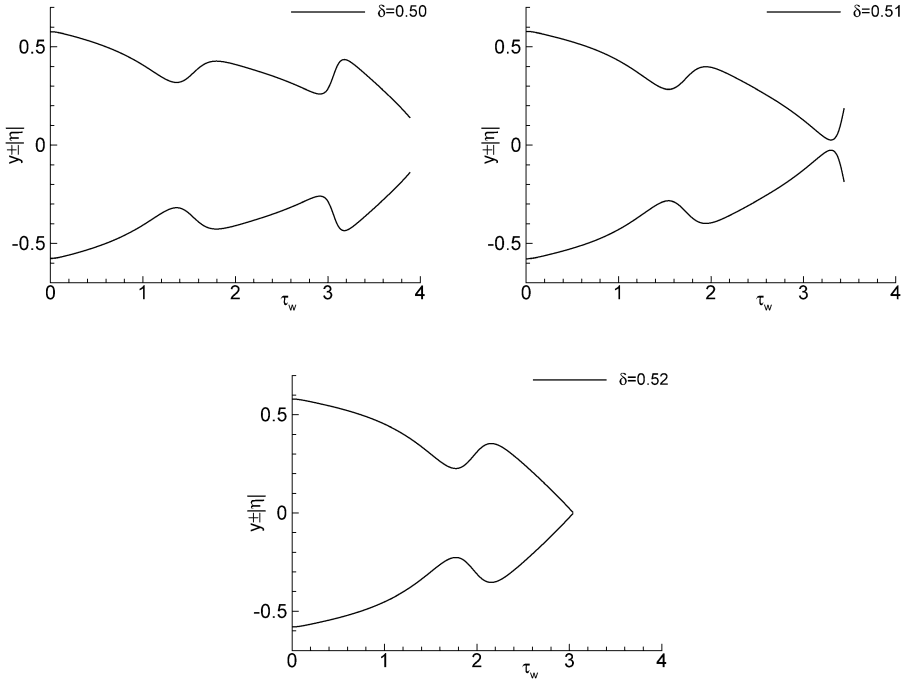

Fig. 14. Inboard extreme of tip vortex positions with perturbations superimposed for the conditions ($\alpha = 0.8$, $\Gamma = 0.2$, $\varepsilon = 0.05$). Breakup occurs when vortices touch at $y = 0$.

The stability results can be used to estimate the time at which the vortices will breakup into rings. This breakup time will depend on the circulation ratio Γ, the spacing parameter δ, the wavenumber α, and the initial perturbation amplitude. The breakup time can be estimated by monitoring the minimum separation between the tip vortices—including the changing vortex positions and the growing perturbations. Given the time dependent tip-vortex positions and the tip-vortex perturbation amplitudes, the inboard extremes for perturbed tip vortices are described by $y_1 + \eta_1$ and $y_2 - \eta_2$. Fig. 14 shows the inboard extremes of the tip vortices as a function of time for $\delta = 0.50$, 0.51, and 0.52, corresponding to $\bar{\delta}_z = 0.77$, 0.81, 0.86, respectively. The circulation ratio, wavenumber, and initial amplitudes are the same as in Fig. 13. The stability results would predict a breakup into rings at $\tau \approx 3.5$ for $\delta = 0.51$. For larger values of δ, the time to breakup will be smaller. A smaller value of δ results in a longer time to breakup. For $\delta = 0.50$, the breakup would occur after $\tau = 4$; since this is after one rotation period, the flap vortices are not likely to continue to play a role in the amplification. To accurately model this stage, the stability analysis must be modified. The general trends predicted by the stability theory are consistent with experimental observations.

7. Conclusions

Trailing vortices are an unavoidable by-product of airplane flight that can result in severe upsets to other airplanes which might encounter them. This has motivated efforts aimed to reduce or alleviate the potential for vortex-encounter upsets.

Studies have shown that vortex-encounter upsets can be dramatically reduced through vortex control. Vortex breakup, via active control, leads to the formation of vortex rings. Flight-simulator studies show that encounters with vortex rings lead to much smaller bank angles for an encountering aircraft compared to straight vortices. Vortex modifications that reduce the strength and increase the diameter via passive control could also reduce the level of upset experienced by an encountering aircraft. However, flight-simulator results suggest that this may require greater than a 50% reduction in the vortex strength (even accounting for an increase in the vortex-core size, and a small amount of waviness).

Detailed studies have shown that vortex breakup can be achieved on vortex systems typical of flaps-down configurations. The breakup effectiveness is linked to simple parameters that describe the vortex system after the rather-complex interactions of the near field. The most significant parameter is a measure of the relative spacing between the flap and tip vortices. A theoretical model for trailing-vortex instabilities is generalized to account for vortex parameters that are typical of more complex vortex systems. The stability theory provides a guide to selecting control parameters, and for assessing the potential effectiveness of

using control. The practical application of any control concepts will require that they have a minimal impact on the overall performance of the airplane, and that they are effective under varied atmospheric conditions.

Acknowledgement

This paper has been influenced by my long-running collaborations with Gregory Miller and Philippe Spalart. I am grateful to Michael Czech, Philippe Spalart, Gregory Miller, and Ömer Savaş for reviewing the manuscript.

References

[1] J.D. Jacob, Ö. Savaş, Vortex dynamics in trailing wakes of flapped rectangular wings, AIAA Paper No. 97-0048, 1997.
[2] J.D. Crouch, G.D. Miller, P.R. Spalart, Active-control system for breakup of airplane trailing vortices, AIAA J. 39 (2001) 2374–2381.
[3] M.J. Czech, G.D. Miller, J.D. Crouch, M. Strelets, Near-field evolution of trailing vortices behind aircraft with flaps deployed, AIAA Paper No. 2004-2149, 2004.
[4] D.A. Durston, S.M. Walker, D.M. Driver, S.C. Smith, Ö. Savaş, Wake vortex alleviation flow field studies, AIAA Paper No. 2004-1073, 2004.
[5] S.C. Crow, Stability theory for a pair of trailing vortices, AIAA J. 8 (1970) 2172–2179.
[6] S.C. Crow, Panel discussion, in: J. Olsen, A. Goldburg, M. Rogers, (Eds.), Aircraft Wake Turbulence and Its Detection, 1971, pp. 551–582.
[7] S.C. Crow, E.R. Bate, Lifespan of trailing vortices in a turbulent atmosphere, J. Aircraft 13 (1976) 476–482.
[8] A.J. Bilanin, S.E. Widnall, Aircraft wake dissipation by sinusoidal instability and vortex breakdown, AIAA Paper No. 73-107, 1973.
[9] J.D. Crouch, Stability of multiple trailing-vortex pairs, AGARD-CP-584, 1996, pp. 17-1–17-8.
[10] J.D. Crouch, Instability and transient growth for two trailing-vortex pairs, J. Fluid Mech. 350 (1997) 311–330.
[11] S.C. Rennich, S.K. Lele, A method for accelerating the destruction of aircraft wake vortices, J. Aircraft 36 (1999) 398–404.
[12] D. Fabre, L. Jacquin, Stability of a four-vortex aircraft wake model, Phys. Fluids 12 (2000) 2438–2443.
[13] D. Fabre, L. Jacquin, A. Loof, Optimal perturbations in a four-vortex aircraft wake in counter-rotating configuration, J. Fluid Mech. 451 (2002) 319–328.
[14] J. Ortega, Ö. Savaş, Rapidly growing instability mode in trailing multiple-vortex wakes, AIAA J. 39 (2001) 750–754.
[15] L. Jacquin, D. Fabre, P. Geffroy, E. Coustols, The properties of a transport aircraft wake in the extended near-field: an experimental study, AIAA Paper No. 2001-1038, 2001.
[16] S. Haverkamp, G. Neuwerth, D. Jacob, Active and passive vortex wake mitigation using control surfaces, Aero. Sci. Tech. 9 (2005) 5–18.
[17] V.J. Rossow, Lift-generated vortex wakes of subsonic transport aircraft, Prog. Aero. Sci. 35 (1999) 507–660.
[18] E. Coustols, E. Stumpf, L. Jacquin, F. Moens, H. Vollmers, T. Gerz, Minimized wake: a collaborative research programme on aircraft wake vortices, AIAA Paper No. 2003-0938, 2003.
[19] P.R. Spalart, Airplane trailing vortices, Annu. Rev. Fluid Mech. 30 (1998) 107–138.
[20] S. Ragab, M. Sreedhar, Numerical simulation of vortices with axial velocity deficits, Phys. Fluids 7 (1995) 549–558.
[21] R. Stuff, The near-far field relationship of vortices shed from transport aircraft, AIAA Paper No. 2001-2429, 2001.
[22] J.M. Ortega, R.L. Bristol, Ö. Savaş, Experimental study of the instability of unequal-strength counter-rotating vortex pairs, J. Fluid Mech. 474 (2003) 35–84.
[23] R.J. Sammonds, G.W. Stinnett Jr., W.E. Larsen, Wake vortex encounter hazard criteria for two aircraft classes, NASA TM-X73113, 1976.
[24] R.E. Loucel, J.D. Crouch, Flight-simulator study of airplane encounters with perturbed trailing vortices, J. Aircraft 42 (2005), in press.
[25] J.D. Crouch, G.D. Miller, P.R. Spalart, Simplified modeling for flaps-down airplane trailing vortices, Bull. Am. Phys. Soc. 46 (2001) 159.